Contrasting Structure-Property Relationships in Amorphous, Hierarchical and Microporous Aluminophosphate Catalysts for Claisen-Schmidt Condensation Reactions

Hamza Annath,*[a,b] Jinesh C. Manayil,[c] Jillian Thompson,[a] Andrew C. Marr,*[a] Robert Raja*[b]

[a]School of Chemistry and Chemical Engineering, Queen's University Belfast, David Keir Building, Stranmillis Road, Belfast BT9 5AG, United Kingdom. Corresponding author, E-mail: h.annath@qub.ac.uk (AH), Correponding author, Tel: +44 (0)28 9097 4442, E-mail: a.marr@qub.ac.uk (AM).

[b]School of Chemistry, University of Southampton, Highfield, University Road, Southampton SO17 1BJ, United Kingdom. Tel: +44(0)23 8059 2144; E-mail: R.Raja@soton.ac.uk.

[c]Energy and Bioproducts Research Institute, College of Engineering & Physical Sciences, Aston University, B4 7ET, Birmingham.

ABSTRACT

Amorphous aluminophosphates are industrial catalysts that are active in aldol-type condensations, dehydration and alkylation. The intrinsic nature of the active sites present in these materials is poorly understood. Herein we report a comparative investigation of the catalytic active sites in amorphous and crystalline aluminophosphates (AFI topology) and their corresponding iron-containing analogues, employing Claisen-Schmidt condensation of acetophenone and benzaldehyde as the test reaction. Secondary porosity generated via the soft-templating approach in hierarchically-porous HP FeAlPO-5, and the presence of large

mesopores in amorphous Am FeAlPO resulted in improved mass-transport and high conversion of carbonyls. The nature and concentration of the active acidic sites within these materials were characterized by pyridine-DRIFTS and propylamine-TPD studies and was shown to play a crucial role in the activation of carbonyl groups and better catalytic performance. Am FeAlPO(5) nearly outperformed HP FeAlPO-5, thus providing a promising alternative for expanding scope in industrial and pharmaceutical applications.

Keywords: Aluminophosphate, Amorphous and crystalline catalysts, Hierarchically porous, Chalcones, Claisen-Schmidt condensation.

1. Introduction

Many of the scientific insights and advances in heterogeneous catalysis and allied technologies gained so far come from the focused and detailed study of catalytic sites within crystalline, single crystal, microporous and ordered materials. This contrasts with the industrial reality, as many industrial catalysts are amorphous materials such as amorphous silica, and silica-alumina as these materials are significantly cheaper [1, 2]. In addition, the amorphous catalyst supports can also show improved performance, compared to their crystalline counterparts, due to their greater flexibility. This flexibility enables them to stabilize different structures of reactants/clusters by adjusting position of atoms and maximising interactions between the host and guest molecules. In contrast to the crystalline materials, the lack of long-range order, complexity of their composition and intrinsic structural heterogeneity of amorphous materials is a barrier to understanding the nature of the active sites present in these materials and their influence on the outcome of a reaction [3]. Nevertheless a few attempts in this regard have been made by employing

computational modelling to reactions on silica, alumina and silica-alumina supported catalysts [4, 5]. It is assumed that the amorphous oxides possess ordered structural arrangements similar to the crystalline counterparts but over a much smaller range. For instance, it is envisaged from the modelling studies of amorphous silica, that there exists a mixture of different crystalline units of β-cristobalite. Though the local structural environment of Si was matched by these models, the siloxane ring or the conventional silanol type distribution were not explained [6, 7]. The incompletely condensed silsesquioxanes model, generated based on above studies, also did not show any similarities to that of amorphous silica. Further modelling studies on amorphous alumina and silica alumina have resulted in more questions rather than reaching a conclusion on their structures [1]. Amorphous silica-alumina is also a widely used catalyst support possessing both Lewis and Bronsted acidic sites formed by the presence of excess Al species and by isomorphic substitution of Al^{3+} for Si^{4+} respectively [8]. It is widely assumed that its structure consists of mixed oxides of silica and alumina rather than a simple physical mixture of oxides.

Amorphous aluminophosphates (Am AlPO) and metal-aluminophosphates (Am MAlPO) are widely applied heterogeneous catalysts, which are cheaper and can possess higher thermal stability compared to their crystalline counterparts [9]. The preparation of these materials involves a simple co-precipitation step. This contrasts with the synthesis of crystalline zeolites and aluminophosphates, which require structure directing organic agents, such as trialkylamines, quarternary ammonium salts, copolymers and organosilanes, which are burnt off post-synthesis. Nagaraju and co-workers studied the weakly acidic and

basic properties of Am AlPO and Am MAlPOs, which are catalytically active for many industrially important organic transformations such as alkylation, trans-esterification, dehydration, and aldol condensation [9-11]. Recently the same authors investigated the physico-chemical properties and catalytic use of Am MAlPOs in aldol condensation of n-heptanal and benzaldehyde to yield jasminaldehyde [12]. Of the different metals studied (Cu, Zn, Cr, Fe, Ce and Zr), Am FeAlPO exhibited the highest activity and selectivity to jasminaldehyde with the conversion of n-heptanal increasing by 60 % and jasminaldehyde selectivity by 30 % when Am FeAlPO was used as a catalyst compared to the bare Am AlPO. The synergistic effect of an optimum amount of both the acid sites and basic sites present on FeAlPO materials, played a significant role in improving the catalytic activity and selectivity. Though some of the structural and catalytic properties of amorphous aluminophosphates have been studied by different groups, a comparative investigation with corresponding crystalline counterparts is not available in literature. However, it is worthy to note the work of A. M. Marquez and Co-workers who have attempted to study the geometric and electronic structures of amorphous aluminophosphates focusing on the effect of the Al/P ratio varied during their synthesis. The ab initio studies, supported by different spectroscopic analyses proposed a short-range order for amorphous aluminophosphates based on metaphosphate anions connected by layers rich in aluminium with a γ-alumina structure [13].

In recent decades, there has been significant progress in the rational design of heterogeneous catalysts containing easily accessible, surface-active sites which are selective towards a target product, contributing to the growth of greener/environmentally

friendly production technologies [14, 15]. However, the design of an efficient solid catalyst for aldol type condensation is still in an advancing stage, despite much interest in fine chemical synthesis and biomass conversion methodologies [16]. Claisen-Schmidt condensation is a cross-aldol condensation of an aldehyde or a ketone having an α-hydrogen with an aromatic carbonyl compound lacking α-hydrogens (Scheme 1) [17]. Chalcone (1,3-diphenylpropenones), a Claisen-Schmidt condensation product, is a valuable organic intermediate and is the basic structural moiety used in the synthesis of heterocyclic ring compounds such as cyanopyridines, pyrazolines, isoxazoles and pyrimidines [17, 18].

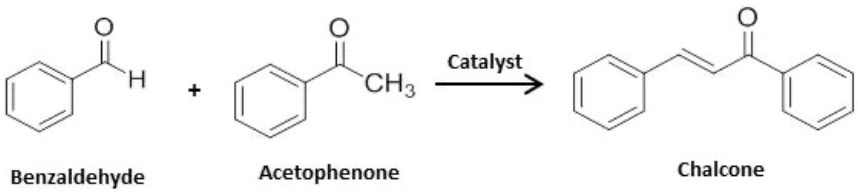

Scheme 1. Reaction of benzaldehyde and acetophenone to form chalcone.

Conventional methods used for producing chalcone are based on homogeneously catalysed reactions via condensation of aromatic carbonyl compounds, mainly acetophenone and benzaldehyde or their derivatives, using stoichiometric amounts of alkali hydroxides or mineral acids [16]. A few solid basic oxides such as MgO, BaO, alkali exchanged zeolites, and hydrotalcites have been used as alternative catalysts [19, 21]. However, the limitations of using solid basic oxides include their low stability at high temperatures and loss of selectivity to chalcone due to the competing Cannizzaro reaction of the aldehyde and/or undesirable Michael addition at strongly basic sites [22, 23].

Attempts have been made to prepare modified solid base catalysts to improve performance by altering the nature of basic sites [24 - 26]. Though the presence of mounted basic sites available in the vicinity of acid sites in these modified base catalysts resulted in enhanced catalytic activity and selectivity, catalyst decay occurred at higher reaction temperatures along with the poisoning of the strongly basic sites. Recently Lewis acidic zeolites such as Sn-modified zeolites have also received attention as catalysts for carbonyl activation and in bio-mass conversion [27 - 31]. Kikhtyanin and co-workers reported the combined role of Lewis acid sites and weak Brønsted acid sites in metal organic frameworks (MOFs) such as FeBTC and CuBTC, in catalysing the aldol condensation of furfural with acetone [32]. The synergistic catalytic role of surface hydroxyl groups, especially silanols has also been explored in aldol type condensation. For instance, Collier et al. reported aldol condensation using amine functionalized MCM-41, in which reaction was cooperatively catalysed by acidic surface hydroxyls and basic amine sites [33]. The aminosilica with capped silanols required a high temperature to initiate the reaction, which is indicative of the ineffective carbonyl activation.

Herein, a comparative investigation of the structural and catalytic performance of amorphous and crystalline (AFI topology; AlPO-5) aluminophosphates and their Fe-containing analogues in the Claisen-Schmidt condensation of benzaldehyde and acetophenone is reported. The diffusional limitations in the microporous crystalline AlPO-5 were taken into consideration and inter-connected mesopores in the form of hierarchical porosity, created by a dual-surfactant assisted synthesis, have been introduced. The additional mesopores in these hierarchically porous aluminophosphate (HP AlPO-5)

materials, along with conventional micropores, help to minimize the mass-transfer limitations for bulkier subtrates/products and provide high specific surface area to achieve isolated and accessible active sites [34]. The nature of the different acidic and basic identify and quantify different acidic and basic sites present in both in the crystalline and amorphous materials along with characterizing their porous properties.

2. Results and Discussion

2.1. Textural and spectroscopic properties of materials

Aluminophosphate and iron containing aluminophosphate in both amorphous and AFI forms (AlPO-5) have been synthesised by co-precipitation and surfactant assisted/hydrothermal synthesis methods, respectively. The detailed preparation methods have been given in the electronic supplementary information (ESI) and the list of materials prepared in the present work is outlined in Table 1. To investigate the textural properties of these materials, adsorption-desorption studies were carried out using nitrogen adsorption at liquid-nitrogen temperature. The BET surface area and micropore and mesopore volumes are presented in Table 1. While microporous AlPO-5 possessed a lower surface area of 209 m^2/g, the corresponding hierarchically porous material (HP AlPO-5) exhibited a surface area of 325 m^2/g and a pore volume of 0.271 cm^3/g, which is consistent with the literature reports of 315 m^2/g and 0.3 cm^3/g [34]. The use of a bulkier surfactant, namely dimethyloctadecyl(3-trimethoxysilylpropyl)ammonium chloride (DMOD), enabled the formation of a large amount of mesopores, alongside the conventional micropores in the frame-work of HP AlPO-5 [34]. Another advantage of HP type materials is the presence of a considerable amount of accessible silanol groups pendant to the mesopore walls, which

resulted from the condensation of the methoxysilyl end of the surfactant DMOD and the surface hydroxyl groups available in the material during the calcination process. While the coprecipitated FeAlPO-5 possessed almost similar surface area and pore volumes compared to the bare AlPO-5, the coprecipitated HP FeAlPO-5 exhibited significantly lower BET surface area and pore volume values compare to the bare HP AlPO5. Am AlPO materials exhibited lower surface area due to the lack of microporosity, but the presence of significant inter-particle spacing in their network structure led to higher pore volume, as reported in literature [9]. As it was reported in the literature [12], the BET surface area of metal incorporated amorphous aluminophosphates (Am MAlPOs) in comparison to a pure Am AlPO are generally higher. Similarly we observed a higher surface area for Am FeAlPO than that of the Am AlPO. While the BET surface area exhibited by Am FeAlPO was 191 m2/g, the surface area exhibited by Am AlPO was only 162 m^2/g. In addition to the surface area values by BET method, we have also calculated the surface by the Density Functional Theory (DFT) model. The results are presented in Table S1. It is interesting to note the a similar trend in the surface area calculated by the DFT model.

The N_2 adsorption-desorption isotherms of the materials are compared and presented in Figure 1. Both the crystalline AFI and amorphous materials exhibited type-IV isotherms with hysteresis loops, indicating the presence of a porous structure [35]. Although both systems are porous in nature, the difference in type and extent of porosity is evident from the corresponding isotherms. The isotherms of AlPO-5 and Fe AlPO-5 show a high adsorption at low P/P_0 typical of microporous solids. In HP materials, the isotherms possess an enhanced N_2 adsorption due to the presence of additional mesopores. The higher

gas intake and a steep adsorption curve at high P/P_0 observed in Am AlPOs, is attributed to the large mesopores arising from inter-particle spaces and the network structure present in these materials [12]. The clear difference in the pore size distribution (PSD) between zeolitic and amorphous aluminophosphates (Figure S1) is worthy of note. Both microporous and HP type AlPO-5 exhibited a narrow PSD. A significant amount of mesopores centred on 5nm are available in the HP materials, which are not observed for microporous AlPO-5 and FeAlPO-5. HP FeAlPO-5 exhibited more uniform pore sizes than bare HP AlPO-5. In contrast Am AlPO and Am FeAlPO(5) materials exhibited a broad PSD curve which indicates the presence of an array of irregular mesopores in these materials. These mesopores are attributed to the inter particle volumes between $AlPO_4$ particles after the condensation of hydroxyl groups [12, 36].

The Powder X-Ray Diffraction (PXRD) patterns of the materials were recorded to evaluate the phase-purity (Figure 2). The crystalline aluminophosphates, irrespective of microporous and HP type, exhibited the intense peaks of the AFI framework as reported in the literature [34]. The Am AlPO and Am FeAlPO(5) are characterized by an amorphous pattern with a broad peak between the 2θ values of 20 to 25 °, characteristic of amorphous materials with fine particles [12]. No peaks associated with iron oxides have been observed in any of the materials studied.

The diffuse reflectance UV-Vis (DRUV) spectra have been recorded for AFI and amorphous, aluminophosphates and iron-aluminophosphates, to investigate the coordination environment of Fe in these materials (Figure S2). The bare samples without Fe showed negligible absorbance in the spectra. However, both the amorphous and crystalline

Fe containing aluminophosphates, exhibited a single intense and broad band around 255 nm. This corresponds to charge-transfer between O^{2-} and Fe^{3+} (ligand to metal) which confirms the tetrahedral geometry of Fe^{3+} [37]. Notably, no peaks were observed after 400 nm for the Am AlPOs, which indicates the absence of any Fe clustering in these materials. The FeAlPO-5 and HP FeAlPO-5 exhibited weak absorption after 400 nm, indicating slight clustering of Fe species and the presence of the tetrahedral geometry of Fe, indicative of the crystalline (AFI) structure [37].

2.2. Acidic properties of materials

Before investigating the type of acidic sites present in these materials, we thought it would be helpful to uncover the type of surface hydroxyl groups present in these materials. The IR spectra were recorded after heating these materials at 150 ˚C *in situ* and bands in the hydroxyl region were examined. The results are presented in the ESI (Figure S3). Both amorphous and AFI aluminophosphates exhibited free P-OH groups at 3675 cm^{-1} [38]. The O-H stretching bands at 3745 cm^{-1} in HP AlPO-5 and HP FeAlPO-5 correspond to the terminal silanol groups, which are not observed in amorphous materials. Am FeAlPO(5) exhibited a weak signal at 3655 cm^{-1} corresponding to free Al-OH groups of defect sites.

To investigate the type of acidic sites, pyridine has been used as a probe molecule and the Diffuse Reflectance Infra-Red (DRIFT) spectra were recorded after careful treatment of the samples with pyridine. The corresponding DRIFT spectra in the range of 1400 to 1650 cm^{-1} are presented in Figure 3A. Characteristic bands, corresponding to the interaction of pyridine molecules with Lewis acidic sites, were observed. The peaks at 1448 and 1490 cm^{-1} correspond to ring C-C stretching bands of pyridine molecules

coordinated with strong Lewis acid sites, as reported in the literature [39]. The presence of extra framework aluminium and/or the high number of defect sites are believed to be the reason for the formation of Lewis acid sites in these materials. The band around 1585 cm^{-1} corresponds to physically bonded pyridine and the one around 1620 cm^{-1} corresponds to hydrogen bonded pyridine to non-acidic hydroxyl groups [39]. It is interesting to point out that the band due to hydrogen bonded pyridine is better resolved and broader in amorphous materials indicating a significant amount of non-acidic hydroxyl groups.

The total surface acidity of the materials was evaluated by propylamine (PA) TPD (Figure 3B). The adsorbed PA undergoes Hoffmann type elimination to form propylene and ammonia at higher temperatures on material surfaces containing acid sites [40]. The signal at m/z 41 in the MS is due to propylene. The decomposition temperature range of PA (decomposition of PA and desorption of reactively formed propene) depends on the strength of acid sites present on the surfaces. The lower the temperature of decomposition of PA (or elimination of propylene), the stronger the acidic sites present on the surface. The total acidity values are given in Table 1. The total number of moles of acid sites is calculated from the corresponding weight loss from the TG-MS. FeAlPO-5 possessed the lowest number of acidic sites, whereas the Am FeAlPO(5) contained the highest number of acid sites. The trend of concentration of total surface acid sites was as follows:

FeAlPO-5 < AlPO-5 < Am AlPO < HP AlPO-5 = HP FeAlPO-5 < Am FeAlPO(5).

Although no significant changes in the concentration of surface acidic sites were observed after introduction of Fe to the aluminophosphates as evidenced from TPD, the number of acidic sites was found to be slightly higher in Am FeAlPO(5)at X mmol/g compared with Y

mmol for Am AlPO. In the case of AFI structures, the concentration of the surface acid sites was either not changed or slightly decreased after the introduction of Fe.

The MS signals corresponding to the formation of propylene after decomposition of PA have been given in Figure 3B. It is interesting to note that the temperature range at which PA decomposition takes place is clearly different for AFI and Am AlPOs. While PA decomposes at a lower temperature (~390 $^{\circ}$C) in Am AlPOs, its decomposition happens at a higher temperature (~450 $^{\circ}$C) range in AFI materials. This indicates that the surface acid sites available in amorphous materials are slightly stronger than that present in AFI aluminophosphates. The microporous AlPO-5 and FeAlPO-5 possess slightly stronger acid sites when compared to the HP AlPO-5 and HP FeAlPO-5. Interestingly, no remarkable temperature difference was observed between Am AlPO and Am FeAlPO(5), thus the results confirmed that introduction of Fe did not enhance the acid strength of AlPOs. Additionally, the crystalline AFI materials exhibited slight basicity as determined by CO2 pulse chemisorption with the amorphous AlPOs contain no basicity at all which is evident from Table 1.

Further investigation of the type of acidic sites was conducted using deuterated acetonitrile (CD_3CN) as a probe molecule, as this small molecule can interact with almost all the available acidic sites and hydroxyl groups present on the surface. The characteristic IR vibrations of nitrile species which interacted with the acidic sites was monitored at different desorption temperatures. The IR spectra of CD_3CN treated aluminophosphates and iron-aluminophosphates are presented in Figure 4. The characteristic bands were observed in the 2100 to 2400 cm^{-1} range. The main bands observed in HP AlPO-5 are at 2285, 2279,

2267 and 2113 cm^{-1}. While the broader signals at 2279 cm^{-1} are attributed to the interaction of nitrile groups with silanols and hydroxyls which are slightly acidic, the band at around 2267 cm^{-1} is attributed to vibrations of CN in liquid-like CD_3CN as reported in the literature [41]. The signal intensity of these bands is high at higher doses of CD_3CN and at low temperature. However, the intensity decreases with increasing temperature in the DRIFT cell due to slow evaporation and desorption of CD_3CN. Interestingly, at 150 °C the bands were not visible. A weak signal appeared at 2308 cm^{-1} for HP FeAlPO-5, which is attributed on weak Lewis acidic sites. The band observed at 2113 cm^{-1} is attributed to the $\nu_{sym}(CD_3)$ mode of vibrations in liquid-like CD_3CN and this peak, along with that at 2267 cm-1 were found to decrease in intensity at lower temperatures than those associated with adsorbed species. The Am AlPO and Am FeAlPO(5) possessed intense signals at 2280 cm^{-1}, indicating the strong interaction of CD_3CN with hydroxyl groups, which is in accordance with the observation from pyridine-DRIFT studies where the peak corresponding to hydrogen bonded pyridine to the non-acidic hydroxyl groups was predominant. It is also noted that these amorphous materials exhibited a vibration band at 2323 cm^{-1}, characteristic of weak Lewis acid sites [42].

2.3. Catalytic activity of materials

The catalytic performance of the materials in the liquid phase Claisen-Schmidt condensation of acetophenone and benzaldehyde was investigated in solvent free condition in a batch reactor at 140 °C for 6h (Table 2). The results are presented in the form of % conversion of acetophenone and % selectivity to chalcone. In all the runs, trans-chalcone was identified as the only product formed by condensation of acetophenone and

benzaldehyde and no self-condensation of acetophenone was identified. Thus 100 % selectivity to trans-chalcone was achieved for all the materials tested. While FeAlPO-5 exhibited the lowest conversion of acetophenone (8 %), Am FeAlPO(5) exhibited the highest conversion (83 %). The catalytic activity was shown to significantly increase from the microporous to hierarchically porous materials, which could be due to the presence of additional mesopores and the acidic nature of silanols present in the mesopores, as evidenced from the IR spectra (Fig S3) and as previously postulated [34]. Consequently, the hierarchically porous HP AlPO-5 displayed higher catalytic activity than that of microporous AlPO-5. The acetophenone conversion was substantially improved, relative to FeAlPO-5, for HP FeAlPO-5, being 8% and 70 % respectively. In addition to this, the effect of Fe content in HP and amorphous materials was clearly evident (Table 2). HP FeAlPO-5 and Am FeAlPO(5) exhibited a two-fold increase in catalytic activity, when compared with corresponding un-doped bare aluminophosphates. The effect of Fe content on the catalytic performance are clearly visible when we compare identical aluminophosphates (in terms of porosity). For example the catalytic performance of HP ALPO-5 has been doubled when there is Fe in the structure. Similarly the catalytic performance of Am AlPO has also been nearly doubled when there is Fe in the structure, that is with Am FeAlPO(5) material. However, though the % conversion of acetophenone catalytic performance of microporous ALPO-5 is increased from 8 to 14 to Fe ALPO-5, but as explained before the accessibility of active sites are limited by the smaller pore size and lack of mesopores in it. Thus, both the available mesopores and the Fe species present in the aluminophosphates structure are found to have significant impacts on the catalytic performance in Claisen-Schmidt condensation. The mesopores in HP materials and

disordered porous structure in amorphous materials can help to overcome the diffusion limitations on the reactant and product molecules. The acidic sites (both Lewis and surface silanols) also played a significant role in improving the catalytic activity of the porous Fe-containing aluminophosphates studied in this work. The strong absorption band observed in the UV-VIS spectra at around 255 nm for microporous FeAlPO-5 (Figure S2) clearly implies the presence of isolated Fe tetrahedral species, but an improved conversion of acetophenone is not achieved due to the diffusional constraints imposed by the micropores to the internal Fe centres. A blank reaction without using any catalyst resulted in 6 % conversion of acetophenone under the same reaction conditions. Thus, at this point it can be concluded that even though Fe promotes the catalytic activity, larger pores are essential for good catalytic performance.

2.4. Insight into the reaction mechanism

The mechanistic aspects of carbonyl condensation reactions catalysed by materials which possess Lewis acidity have been well studied [30, 43- 45]. The cooperative role of Lewis acid sites, along with weakly basic framework oxygens linked to the metal, are well understood [31]. The activation of the carbonyl group by metal atoms along with proton abstraction by the basic oxygen attached to the metal leads to formation of a metal-enolate that helps the C-C coupling reaction to proceed. The reported mechanism is given in Scheme S1 in the ESI [31]. The interaction of a Lewis acidic metal atom with the carbonyl makes the α-proton more basic and therefore it can be easily abstracted by the weakly basic oxygen in the framework structure. Si-OH, Al-OH or P-OH are believed to be formed from the abstracted proton, which is then transferred to the intermediate species to form

chalcone. A similar type of proton abstraction and transfer has been explained by Bell and co-workers in the isomerization of glucose to fructose by Beta zeolite [46]. In their work, the high ionicity of the oxygen−metal bond enhances the Brønsted basicity of the oxygen atoms, which, in turn, governs the magnitude of the electrostatic stabilization between the transition state and the active site (Lewis acid sites, in this case). This mechanistic approach can be extended to the present work where all the materials characterized were shown to possess strong Lewis sites. Since the reaction product chalcone is relatively bulky, smooth running of the reaction pathway can only be expected in those aluminophosphates/iron-aluminophosphates which contain a significant amount of mesopores and/or pore volume. The Lewis acid sites in HP and amorphous materials are believed to be more easily accessible and thus catalyse the condensation of benzaldehyde and acetophenone much more efficiently, consistent with the number and strength of acid sites present in these materials. Furthermore, the percentage conversion of acetophenone and the number of moles of acid sites present in the catalyst have been correlated in Figure 5. In addition to this, the normalised acidic sites have been calculated based on the BET surface area of materials (Table S2). The catalyst with the lowest acid site concentration (FeAlPO-5) exhibited the lowest activity and the one with the highest acid site concentration (Am FeAlPO(5)) exhibited the highest activity. The superior performance of Am FeAlPO compared to HP FeAlPO-5 might be due to the stronger surface acidic sites present in these materials as evidenced from PA-TPD investigations. Additionally, the enhanced activity of Am FeAlPO(5) in comparison to Am AlPO can be explained on the basis of the high concentration of Lewis acidic sites resulting from Fe sites, higher pore size and a slightly higher acid-site density.

2.5. Effect of reaction temperature

The effect of reaction temperature on the catalytic performance of Am FeAlPO(5) catalyst was also studied (Figure S4). The percentage conversion of acetophenone in Claisen-Schmidt condensation was found to increase with increasing reaction temperature. The highest conversion achievable with total selectivity was measured at 140 ˚C. Further increases in temperature reduced the selectivity to chalcone, which can be attributed to the formation of higher molecular weight products. 140 ˚C was found to be the optimum temperature for the reaction using the Am FeAlPO(5) as the catalyst. The activation energy calculated based on Figure S4 using Arrhenius equation shows about 40 kJ mol^{-1}. This is higher than that expected for a process under diffusion limitation, further supporting the lack of diffusion limitation through the interparticle volume in this amorphous catalyst.

2.5. Reusability of the catalysts

The reusability of both HP FeAlPO-5 and Am FeAlPO(5) catalysts in chalcone synthesis was examined four times. For this, after the reaction mixture was cooled, the used catalyst was collected by filtration, thoroughly washed with hot toluene and dried at 150 ˚C for 3h, before being used for the next cycle. Both catalysts were found to be recyclable without notable loss of the catalytic activity and selectivity (Figure S5).

3. Conclusion

Microporous/hierarchically porous and amorphous, aluminophosphates and iron aluminophosphates were synthesised and characterized, with emphasis on the porosity and acid sites present. The materials were evaluated as catalysts in the liquid phase Claisen-

Schmidt condensation of acetophenone and benzaldehyde to chalcones. The comparative investigation of these crystalline and amorphous aluminophosphates by spectroscopic and textural methods reveals a remarkable difference in their physico-chemical properties, which can be correlated with their catalytic activity. The catalytic benefits of incorporating Fe in AFI aluminophosphates is clearly reflected in the hierarchically porous material, but not in the microporous analogues. The diffusional constraints in microporous AlPO-5 and FeAlPO-5 is alleviated in hierarchical HP AlPO-5 and HP FeAlPO-5 due to the presence of secondary mesopores, introduced by the soft-templating approach, during synthesis. The amorphous FeAlPO with similar iron content as that of crystalline material, which was synthesised by a co-precipitation method, exhibits a comparable catalytic performance to that of HP AlPO-5. The presence of Lewis acid sites observed from Pyridine-DRIFT studies and the acidity profiles observed from n-propylamine TPD measurements in both amorphous and crystalline FeAlPO suggest that the acid-site density and overall strength of acid sites is important for catalysing the carbonyl condensation in this case. Carbon dioxide-TPD measurements revealed that these materials do not possess any basic sites although the basicity of the structural oxygen is believed to be playing a role in the catalysis, which warrants further investigation. Notably the superior catalytic activity observed with amorphous FeAlPO, which is prepared without employing any structure directing agents, indicates that one can design or mimic analogous catalytic active sites in amorphous catalysts having disordered pores with the same chemical composition to that of the corresponding crystalline and zeolitic materials. This work outlines the scope of designing economical and efficient catalysts for aldol type condensations reactions, which are widely used in many industrial catalytic processes and biomass valorisations.

Acknowledgements

This work was supported by the EPSRC U.K. Catalysis Hub through Grant EP/K014714/1; they are kindly thanked for the resources and support provided via our membership of the U.K. Catalysis Hub Consortium. JCM thanks BBSRC GCRF grant (BB/P022685/1) for financial support.

Appendix. Supplementary data

Electronic Supplementary Information (ESI) available: Experimental procedures, Pore Size Distribution of AFI aluminophosphates and amorphous aluminophosphates, UV-VIS spectra, IR spectra of hydroxyl regions of hierarchically porous and amorphous aluminophosphates, Scheme S1, the effect of temperature on the catalytic performance of Am FeAlPO(5) and the catalyst re-usability data.

References

[1] B.R. Goldsmith, B. Peters, J.K. Johnson, B.C. Gates, S.L. Scott, ACS Catal. 7 (2017) 7543-7557.

[2] R. Zallen, in *The Physics of Amorphous Solids*; Wiley Mörlenbach, **2008**.

[3] C.S. Ewing, M.J. Hartmann, K.R. Martin, A.M. Musto, S.J. Padinjarekutt, E.M. Weiss, G. Veser, J.J. McCarthy, J.K. Johnson, D. S. Lambrecht, J. Phys. Chem. C. 119 (2015) 2503-2512.

[4] A. Fong, Y. Yuan, S.L. Ivry, S.L. Scott, B. Peters, ACS Catal. 5 (2015) 5, 3360-3374.

[5] A. Fong, B. Peters, S. L. Scott, ACS Catal. 6 (2016) 6073-6085.

[6] Chuang, I. S.; Maciel, G. E. J. Phys. Chem. B 1997, 101, 3052− 3064.

[7] Fraile, J. M.; García, J. I.; Mayoral, J. A.; Vispe, E. J. Catal. 2005, 233, 90−99.

[8] Leydier, F.; Chizallet, C.; Costa, D.; Raybaud, P. J. Catal. 2015, 325, 35−47.

[9] A.V. Vijayasankar, N. Mahadevaiah, Y.S. Bhat, N. Nagaraju, J. Porous. Mater., 18 (2011) 369-378.

[10] N. Nagaraju, G. Kuriakose, Green Chem. 4 (2002) 269–271.

[11] A.V. Vijayasankar, S. Deepa, B.R. Venugopal, N. Nagaraju, Chin. J. Catal. 31 (2010) 1321-1327.

[12] A. Hamza, N. Nagaraju, Chin. J. Catal. 36 (2015) 209-215.

[13] Antonio M. Ma´rquez, Jaime Oviedo, Javier Ferna´ndez Sanz, Jose´ J. Benı´tez and Jose´ Antonio Odriozola, J. Phys. Chem. B 1997, 101, 9510-9516.

[14] J. D. A. Pelletier, J-M Basset, Acc. Chem. Res. 49 (2016) 664-677.

[15] V.D. Santo, M. Guidatti, R. Psaro, L. Marchese, F. Carniato, C. Bisio, Proc. R. Soc. A. 468 (2012) 1904-1926.

[16] C. Zhuang, W. Zhang, C. Sheng, W. Zhang, C. Xing, Z. Miao, Chem Rev. 117(12) (2017) 7762–7810.

[17] P.S. Utale, P.B. Raghuvanshi, A.G. Doshi, Asian J. Chem. 10 (1998) 597-599.

[18] S.K. Kumar, E. Hager C. Pettit, H. Gurulingappa, N.E. Davidson, S. R. Khan, J. Med. Chem. 46 (2003) 2813-2815.

[19] M.T. Drexler, M. D. Amiridis, J. Catal. 214 (2003) 136-145.

[20] M. Lakshmi Kantam , B. Veda Prakash, Ch. Venkat Reddy, Synthetic. Commun., 35 (2005) 1971-1978.

[21] A. Corma, M. J. Climent, H. Garcia and J. Primo, Catal. Lett. 4 (1990) 4, 85-91.

[22] A.H. Jadhav, D. Prasad. H.S. Jadav. B.M. Nagaraja, J.G. Seo, Energy 160 (2018) 635-647.

[23] A. Gervasini, A. Auroux, J. Catal. 131 (1991) 190-198.

[24] J.I. Yu, S.Y. Shiau and A. N. Ko, Catal. Lett. 77 (2001) 165-169.

[25] A. Auroux, A. Gervasini, J. Phys. Chem. 94 (1990) 6371-6379.

[26] X.G. Wang, K.S.K. Lin, J.C.C. Chan, S. Cheng, J. Phys. Chem. B. 109 (2005) 1763-1769.

[27] A. Corma, L.T. Nemeth, M. Renz, S. Valencia, Nature 412 (2001) 423-425.

[28] J. Dijkmans, M. Dusselier, D. Gabriels, K. Houthoofd, P.C.M.M. Magusin, S. Huang, Y. Pontikes, M. Trekels, A. Vantomme, L. Giebeler, S. Oswald, B. F. Sels, ACS Catal. 5 (2015) 928-940.

[29] S. Van de Vyver, C. Odermatt, K. Romero, T. Prasomsri, Y. Roman-Leshkov, ACS Catal. 5 (2015) 972-977.

[30] M. Su, W. Li, T. Zhang, H. S. Xin, S. Li, W. Fan, L. Ma, Catal. Sci. Technol. 7 (2017) 3555-3561.

[31] J.D. Lewis, S. Van de Vyver, Y. Román-Leshkov, Angew. Chem Int. Ed. 54 (2015) 9835-9838.

[32] O. Kikhtyanin, D. Kubicka, J. Cejka, Catal. Today 243 (2015) 158-162.

[33] V.E. Collier, N.C. Ellebracht, G.I. Lindy, E.G. Moschetta, C. W. Jones, ACS Catal. 6 (2016), 460-468.

[34] S. H. Newland, W. Sinkler, T. Mezza, S.R. Bare, M. Carravetta, I.M. Haies, A. Levy, S. Keenan, R. Raja, ACS Catal. 5(11) (2015) 6587-6593.

[35] K.S.W. Sing, Pure and Appl. Chem., 54 (1982) 2201-2218.

[36] R. Rosseto, Á.C.M.A. dos Santos, F. Galembeck, J. Braz. Chem. Soc. 17 (2006) 1465-1472.

[37] W. Wei, J.A. Moulijn, G. Mul, Microporous Mesoporous Mater. 112 (2008) 193-201.

[38] K.M.H. Mohammed, A. Chutia, J. Callison, P.P. Wells, E.K. Gibson, A.M. Beale, C.R.A. Catlow, R. Raja, J. Mater. Chem. A. 4 (2016) 5706-5712.

[39] E. Selli, L. Forni, Microporous Mesoporous Mater. 31 (1999) 129-140.

[40] Q. Huo, T. Dou, Z. Zhaoa, H. Pan, Appl. Catal. A: Gen. 381 (2010) 101-108.

[41] B.R.G. Leliveld, M.J.H.V. Kerkhos, F.A. Broersma, J.A.J. van Dillen, J.W. Geus, D.C. Koningsberger, J. Chem. Soc., Faraday T rans., 94(2) (1998) 315-321.

[42] C. Paze, A. Zecchina, S. Spera, G. Spano, F. Rivetti, Phys. Chem. Chem. Phys., 2 (2000) 5756-5760.

[43] A. Dhakshinamoorthy, M. Alvaro, H. Garcia, Adv. Synth. Catal. 352 (2010) 711-717.

[44] Y. Román-Leshkov, M. E. Davis, ACS Catal. 1 (2011) 1566-1580.

[45] R. Bermejo-Deval, R. Gounder, M. E. Davis, ACS Catal. 2 (2012) 2705-2713.

[46] Y. -P. Li, M. Head-Gordon, A. T. Bell, ACS Catal. 4 (2014) 1537-1545.

Table 1 BET surface area, mesopore and micropore volume, acidity and basicity of the materials studied.

Material	Structure	BET Surface Area (m^2/g)	BJH Pore Volume (cc/g)	Micro Pore Volume (cc/g)	Acidity (mmol/g)[a]	Basicity (mmol/g)[b]
AlPO-5	Microporous-AFI	209	0.082	0.081	0.18	0.016
FeAlPO-5	Microporous-AFI	207	0.075	0.074	0.14	0.007
HP AlPO-5	Hierarchically porous- AFI	325	0.271	0.088	0.33	0.006
HP FeAlPO-5	Hierarchically porous- AFI	226	0.136	0.073	0.33	0.002
Am AlPO	Amorphous	162	0.500	-	0.30	Nil
Am FeAlPO(5)	Amorphous	191	0.532	-	0.39	Nil

[a] Propylamine adsorption/TG-MS analysis

[b] CO_2-TPD

Table 2 Percentage conversion of acetophenone and selectivity to chalcone in the condensation of benzaldehyde and acetophenone using amorphous and AFI, aluminophosphates and iron-aluminophosphates.

Catalyst	Conversion of acetophenone (%)	Selectivity of trans chalcone (%)
AlPO-5	14	100
FeAlPO-5	8	100
HP AlPO-5	35	100
HP FeAlPO-5	70	100
Am AlPO	48	100
Am FeAlPO(5)	83	100
Blank	6	-

Reaction Condition: 6.2 mmol acetophenone, 8.1 mmol benzaldehyde, 0.15g catalyst, 140 °C, Solvent free, and 6h duration.

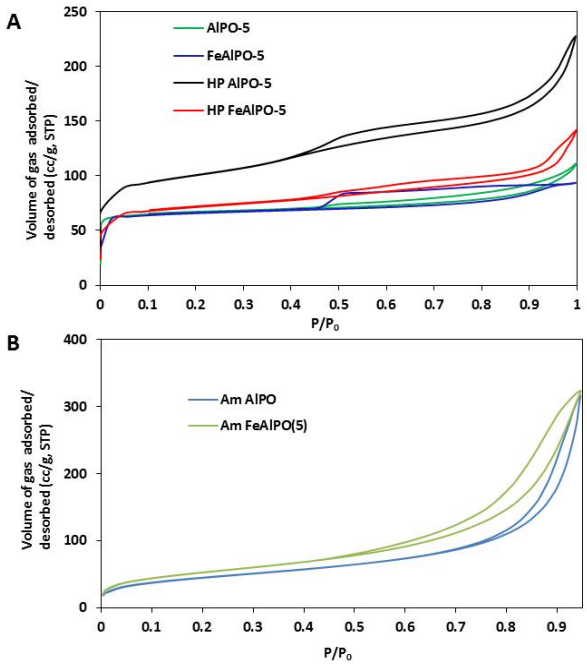

Figure 1. N_2 adsorption-desorption isotherms of a) AFI aluminophosphates; b) amorphous aluminophosphates.

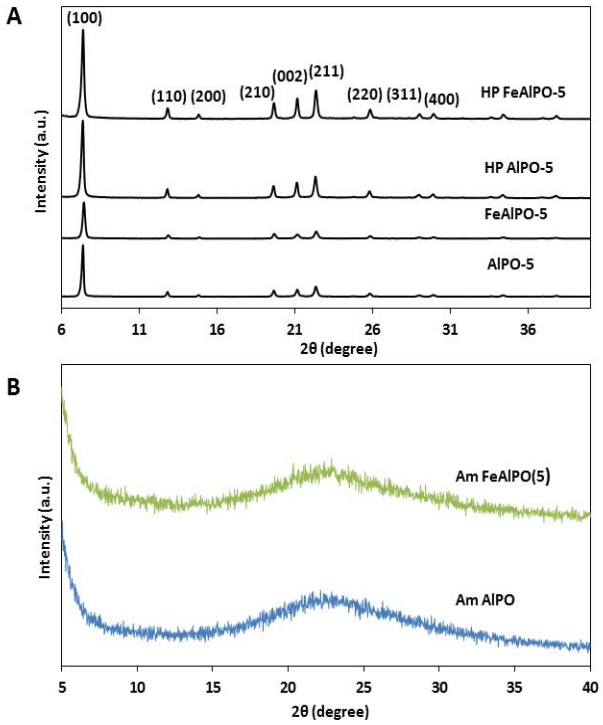

Figure 2. PXRD patterns of a) AFI aluminophosphates; b) amorphous aluminophosphates.

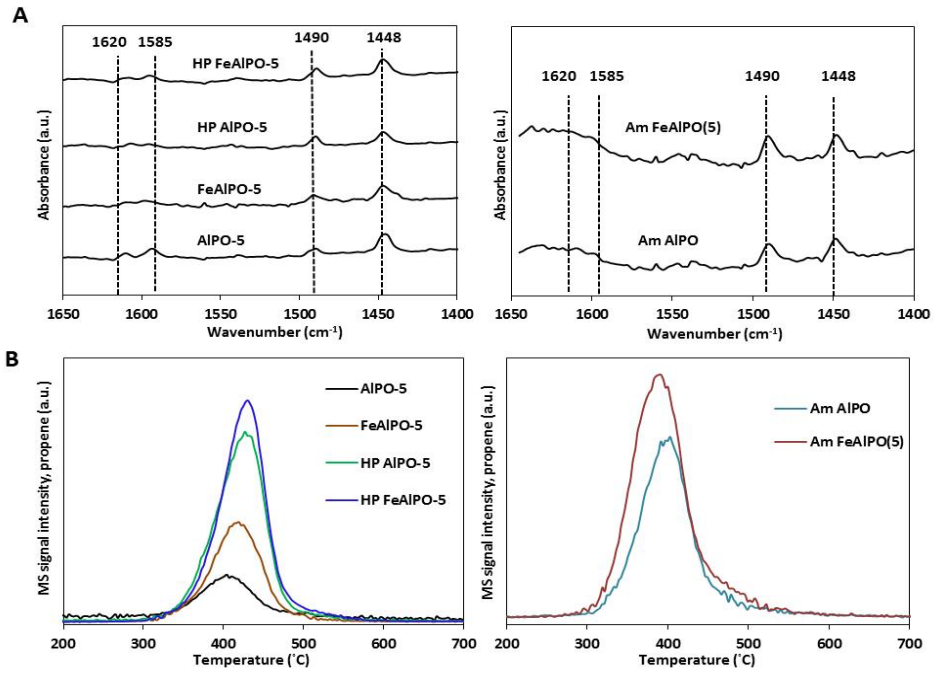

Figure 3. a) Pyridine probed DRIFT spectra; b) propylamine TPD-MS profiles of AFI aluminophosphates and amorphous aluminophosphates.

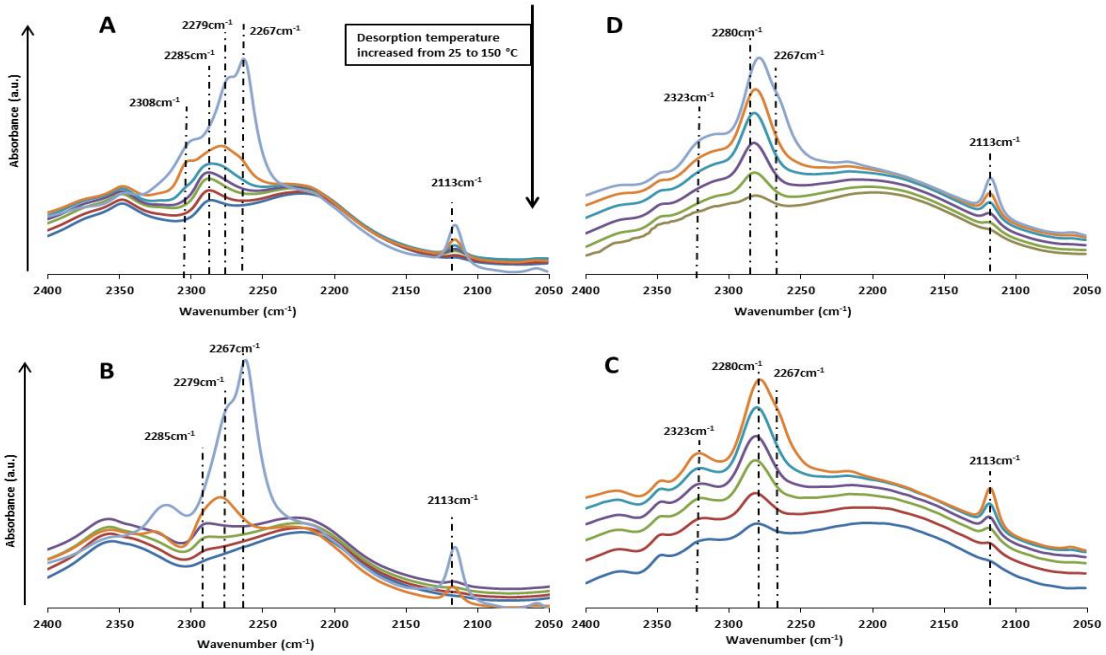

Figure 4. CD_3CN-probed IR spectra of a) HP FeAlPO-5; b) HP AlPO-5; c) Am AlPO; d) Am FeAlPO(5).

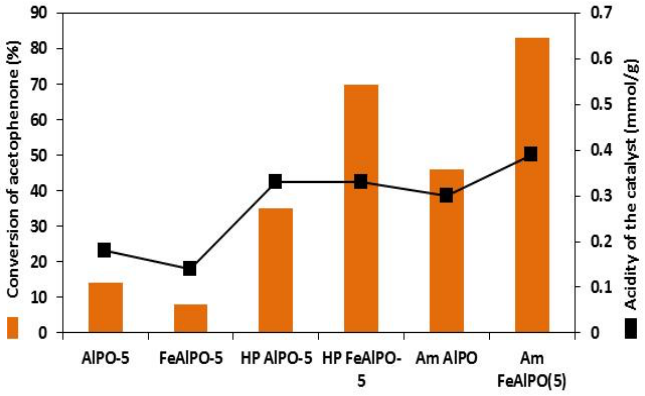

Figure 5. Correlation of the percentage conversion of acetophenone with the total acidity of the catalyst.